JOURNAL OF APPLIED ELECTROCHEMISTRY **29** (1999) 75–80

Electrochemical evaluation of molybdenum nitride electrodes in H_2SO_4 electrolyte

S. L. ROBERSON*, D. FINELLO‡, R. F. DAVIS

Department of Materials Science and Engineering, North Carolina State University, Box 7907 Raleigh, NC 27695-7907, USA

Received 15 August 1997; accepted in revised form 21 April 1998

The electrochemical stability of polycrystalline thin film Mo_xN ($x = 1$ and 2) electrodes deposited on previously *nitrided* polycrystalline Ti and bare Ti substrates and exposed to 4.4 M H_2SO_4 electrolyte has been investigated. The electrodes were prepared by a temperature programmed procedure involving the reaction of MoO_3 films and NH_3. Cyclic voltammetry and a.c. impedance spectroscopy indicated that the range of electrochemical voltage stability in the electrolyte of the Mo_xN films on *nitrided* Ti substrates, referenced to a standard hydrogen electrode to be −0.01 to +0.69 V. These electrodes had a calculated capacitance of about 315 F cm^{-3}. The Mo_xN films on Ti substrates were electrochemically stable from −0.01 to +0.67 V; however, they contained unconverted MoO_2 which acted to reduce the calculated capacitance to about 210 F cm^{-3}. At and above +0.70 V and +0.68 V on *nitrided* Ti and Ti substrates, respectively, an electrochemical reaction occurred. The formation of an amorphous phase in the reacted Mo_xN films was indicated by X-ray diffraction (XRD). Secondary ion mass spectroscopy (SIMS) showed increases in the atomic concentrations of hydrogen, oxygen and sulfur in the reacted films. The voltage bias applied to the electrodes influenced the chemical composition of the reacted films.

Keywords: *molybdenum nitride electrodes*, *capacitors*, *H_2SO_4 electrolytes*

1. Introduction

The numerous potential and realized applications of conductive high surface area (HSA) materials, including catalysts and electrodes in high energy density electrochemical double layer capacitors, have prompted research and development into growth of these materials. At present, either HSA carbon powder or ruthenium oxide is commonly used in the latter application. However, low volumetric energy density values and high equivalent series resistance values limits the use of the former, and the latter material is uneconomical. Alternative candidate materials include the transition metal nitrides M_xN_y (M = Mo, Ti, Ni, V, Cr, or W), which have electrical conductivities exceeding $10^4\,\Omega^{-1}\,cm^{-1}$ and good resistance to electrochemical decomposition in aqueous electrolytes [1]. The material of interest in the present research is molybdenum nitride due to its high electrical conductivity and resistance to electrochemical decomposition. To form high surface area films ($\geqslant 30\,m^2\,g^{-1}$) of this material, it is advantageous to make use of the increase in the crystallographic density which occurs during the conversion of MoO_3 ($\rho \approx 4.69\,g\,cm^{-3}$) to MoN ($\rho \approx 9.05\,g\,cm^{-3}$), and Mo_2N ($\rho \approx 9.50\,g\,cm^{-3}$) [2–5]. This change in density also results in a large increase in surface area caused by the formation of microcracks, pores and cavities since the conversion is associated with a concomitant and significant increase in the bulk density of the nitride.

Several techniques have been used to deposit Mo_xN films [6–8]; however, they have not yielded a material having a small grain size or high surface area. By contrast, Mo_xN films with grain sizes ~20 nm and high surface areas ($> 30\,m^2\,g^{-1}$) have recently been achieved in the authors' laboratories [9]. The availability of these films in the form of electrodes has allowed the determination of the electrochemical stability and reaction products of Mo_xN electrodes in H_2SO_4.

In this research, we have observed that Mo_xN thin film electrodes have a capacitance to 315 F cm^{-3} or ~35 F gm^{-1} and an equivalent series resistance (ESR) value of 0.04 Ω. These films are electrochemically stable in a 4.4 M H_2SO_4 electrolyte between −0.01 and +0.69 V, and −0.01 and +0.67 V on *nitrided* Ti and Ti substrates, respectively. Below and above these values, electrochemical reactions resulted in the formation of an amorphous material, as shown by X-ray diffraction (XRD).

* Correspondence concerning this paper should be directed to S. L. Roberson at US Air Force Research Labs, Munitions Directorate, Building 432 Fuzes Branch, 306 W. Eglin Blvd, Eglin AFB, FL 32542-6810, USA.
‡ US Air Force Research Labs, Munitions Directorate, Eglin AFB, FL 32542-6810, USA.

2. Experimental details

As-received, 50 μm thick polycrystalline Ti substrates, were cut into one inch squares, cleaned sequentially in trichloroethylene, acetone and methanol, etched in 1.0 M HCl at 90 °C for 10 min to remove the surface oxide, rinsed in methanol and dried. Surface nitridation was accomplished by heating the prepared Ti substrates to 700 °C for 1 h in NH_3 flowing at 4 $dm^3\,min^{-1}$ in a quartz lined stainless steel tube furnace which had been previously evacuated to 10^{-3} torr.

The production of MoO_3 films was accomplished in a resistively heated, pancake-style, atmospheric spray pyrolysis deposition system containing a thin layer chromatography (TLC) sprayer to deliver the liquid molybdenum source (5 g of $MoCl_5$/100 ml DI H_2O + 50 ml methanol) to the substrate. The substrates (nitrided Ti or Ti) were heated to 500 °C, and the process sequence initiated by flowing nitrogen at 14 $dm^3\,min^{-1}$ over the liquid inlet of the TLC sprayer. At this flow rate the liquid source was siphoned up the inlet tube, dispersed into fine droplets, and deposited on the substrate. The pyrolysis of the liquid source in air produced MoO_3 on the substrate. The process route for the growth of MoO_3 films employed an on/off cycle involving the deposition of MoO_3 for 30 s and the cessation of the flow of nitrogen (and the deposition) for 30 s. This process was repeated 15 times to prepare 15 μm thick MoO_3 films.

To achieve the conversion of the MoO_3 films to Mo_xN, the former were placed in a quartz lined stainless steel tube furnace and evacuated to 10^{-3} torr. The system was seven times sequentially back-filled with UHP (99.999%) nitrogen to atmospheric pressure and evacuated to 10^{-3} torr to reduce the oxygen level in the system to a minimum. To eliminate any detectable MoO_2 in the Mo_xN films on *nitrided* Ti substrates, the following temperature programmed reaction sequence was developed by the authors and conducted at atmospheric pressure and an NH_3 flow rate of 7 $dm^3\,min^{-1}$: 325 °C h^{-1} from room temperature to 325 °C, 20 °C h^{-1} from 300–580 °C, 160 °C h^{-1} from 580–750 °C and a final soak at 750 °C for 2 h. The resulting Mo_xN films were cooled to room temperature at a rate of 340 °C h^{-1} and passivated for 24 h in nitrogen flowing at 2 $dm^3\,min^{-1}$ to prevent rapid oxidation due to their high surface areas.

The structural, chemical, and surface microstructural properties of the Mo_xN films were analyzed prior to and after electrochemical reaction using several techniques. X-ray diffraction (Rigaku model A) was used to identify the bulk phases. Secondary ion mass spectroscopy (Cameca ims-3F) depth profiling was employed to determine the presence of elements in low concentrations with an Mo_xN film calibrated for H, Mo, N, O, and S via ion implantation being used as the standard for SIMS. Scanning electron microscopy (SEM) (Jeol 6400FE) at 5 kV was used to determine the effects of the electrochemical reaction on the surface microstructure of the films.

The electrochemical evaluation of the Mo_xN electrodes in H_2SO_4 was conducted using cyclic voltammetry (CV) and a.c. impedance spectroscopy in 4.4 M H_2SO_4 on 1 cm^2 samples. The former measurements were taken using a standard hydrogen reference electrode, a platinum counter electrode and an EEG (model 173) potentiostat in tandem with an EEG (model 175) programmer at a scan rate of 10 mV s^{-1}. The capacitance of each of these films was determined by integrating the rectangular area of the CV curves and dividing this value by twice the scan rate. This gives a more accurate and useful capacitance value than instantaneous capacitance measurements, which tend to overestimate the useable capacitance of a given electrode. Capacitance values are reported in F gm^{-1}, F cm^{-2} and F cm^{-3}. This last unit allows for the comparison of this electrode material with other electrode materials of different densities. After the stability limits of the electrodes were determined by CV, a two electrode 'test cell' was constructed from identical but untested samples. These electrodes were then used to perform SIMS depth profiling and XRD studies. This provided a more accurate description of the capacitive behavior of these electrodes in a two electrode cell. A Solotron 1250 frequency analyser and an EEG (Model 273) potentiostat were used for the a.c. impedance studies. These studies were conducted to observe the electrochemical reactions at and near the electrochemical stability limits of the electrodes.

3. Results and discussion

The successful fabrication in this research [9] of Mo_xN films on previously *nitrided* Ti substrates with very low oxygen concentrations has been paramount to the investigation of the electrochemical stability and any resultant reaction products of these films when exposed to 4.4 M H_2SO_4. This is due to the instability of molybdenum oxides in H_2SO_4. A representative XRD pattern of these films prior to electrochemical reaction is shown in Fig. 1(a). The films consisted of ~60% γ-Mo_2N and ~40% δ-MoN. The peak broadening is due to the very small (~10 nm) average grain size. A representative XRD pattern of a film following conversion on a Ti substrate, which had not been nitrided, is shown in Fig. 1(b) for comparison. A bulk MoO_2 phase is present in the latter film due to the incomplete conversion of MoO_3 to Mo_2N near the film/substrate interface. This was found to be related to the formation of TiO on the Ti substrate during the MoO_3 deposition process. It was discovered that once titanium oxides (TiO_2 and TiO) were formed on the substrate, it was thermodynamically impossible at the reaction temperatures and pressures employed to convert these oxides to Ti_2N or TiN. As the Gibbs free energy of formation of MoO_2 possesses a more negative value than TiO at temperatures below 730 °C, the presence of TiO was

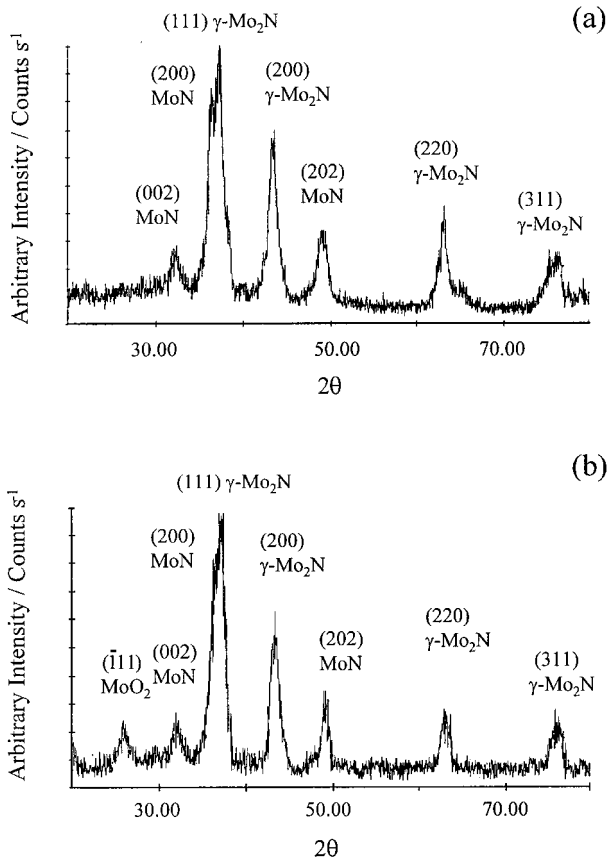

Fig. 1. X-ray diffraction patterns of (a) a low oxygen concentration Mo_xN film on a *nitrided* Ti substrate and (b) a MoO_2 contaminated Mo_xN film on a Ti substrate prior to exposure to H_2SO_4.

found to inhibit the conversion of MoO_3 to Mo_xN. Above this temperature, TiO is thermodynamically more stable than MoO_2. However, attempts to prepare low oxygen concentration Mo_xN films on Ti substrates, which had not been nitrided, were unsuccessful even when the films were held at 790 °C for 10 h after the conversion reaction.

Representative cyclic voltammogram (CV) curves determined for 1 and 50 cycles for an Mo_xN film on a *nitrided* Ti substrate biased at (a) +0.70 V and (b) +0.69 V are shown in Fig. 2. The splitting of the lines between cycles 1 and 50 in (a) indicate a reduction in capacitance which is directly related to a decrease in film thickness due to an electrochemical reaction and resultant etching. In contrast, the overlapping lines of cycles 1 and 50 in (b) indicate that Mo_xN films are electrochemically stable in 4.4 M H_2SO_4 at and below +0.69 V. Although not shown here, subsequent XRD analysis of films exposed below +0.69 V after 500 cycles confirmed that the Mo_xN films were electrochemically stable at this voltage. The rectangular shape of the CV curves indicates that the Mo_xN films are capacitive with a calculated value of $\sim$0.50 F cm^{-2}, 35 F g^{-1} and 315 F cm^{-3}. In Fig. 3, a cyclic voltammogram of an Mo_xN film on a Ti substrate which had not been nitrided biased at (a) +0.68 V and (b) +0.67 V is shown. In (a) the splitting of the lines indicate an electrochemical reaction

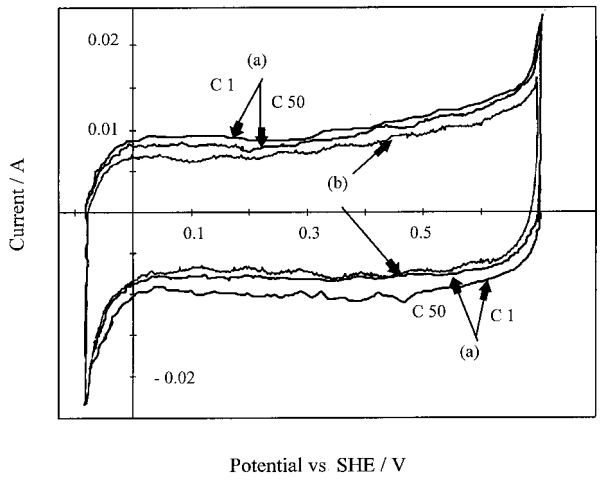

Fig. 2. Cyclic voltammogram for cycles 1 and 50 for Mo_xN electrodes on *nitrided* Ti substrates in 4.4 M H_2SO_4 biased at (a) +0.70 V and (b) +0.69 V. Scan rate 10 m V s^{-1}.

on the film and a reduction in capacitance. In (b) the film is electrochemically stable after 50 cycles and no reaction was observed in this film. These films had lower capacitance values ($\sim$0.35 F cm^{-2}, 22 F g^{-1} and 210 F cm^{-3}) than films deposited on *nitrided* Ti substrates. This reduced value and a related reduction in electrical conductivity are a result of the reduced surface area of the film due to the presence of unreacted MoO_2.

The electrochemical characteristics of Mo_xN films on *nitrided* Ti and Ti substrates determined by a.c. impedance spectroscopy are shown in Fig. 4(a) and (b), and Fig. 5(a) and (b). In Fig. 4(a), the magnitude of the impedance [Z], and capacitance (C), of the Mo_xN electrodes biased at +0.69 V is plotted against frequency. As this Figure indicates, the capacitance of a two-electrode Mo_xN cell at low frequencies approaches 0.70 F cm^{-2}, 49 F g^{-1} and 443 F cm^{-3}. These values do not agree with the capacitance values obtained using cyclic voltammetry. This difference is a result of the use of the rectangular method, which underestimates the capacitance especially in instances

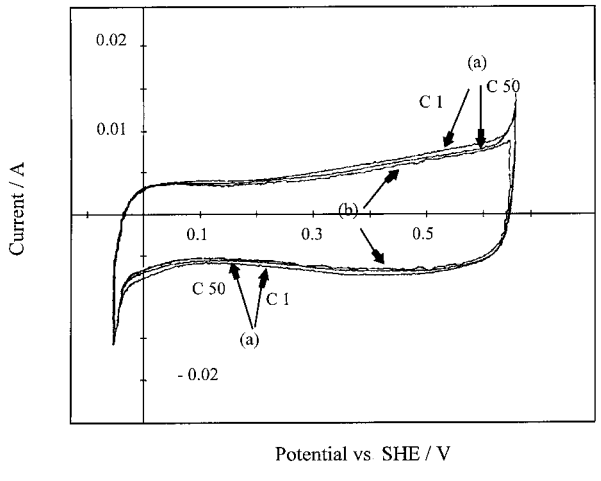

Fig. 3. Cyclic voltammogram for cycles 1 and 50 for Mo_xN electrodes on Ti substrates in 4.4 M H_2SO_4 biased at (a) +0.68 V and (b) +0.67 V substrates. Scan rate 10 m V s^{-1}.

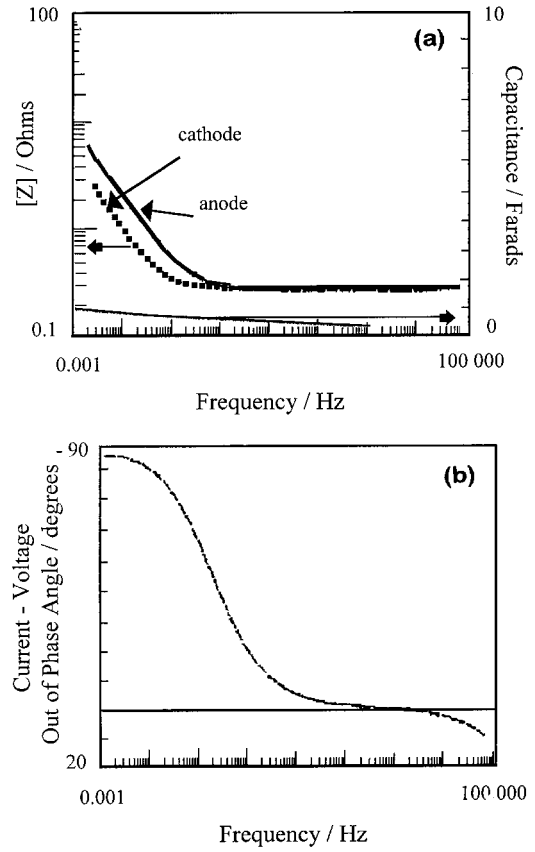

Fig. 4. AC impedance spectroscopy plots of Mo_xN electrodes biased at +0.69 V on *nitrided* Ti substrates in 4.4 M H_2SO_4 showing (a) magnitude of the impedance [*Z*] and capacitance, and (b) current–voltage phase against frequency.

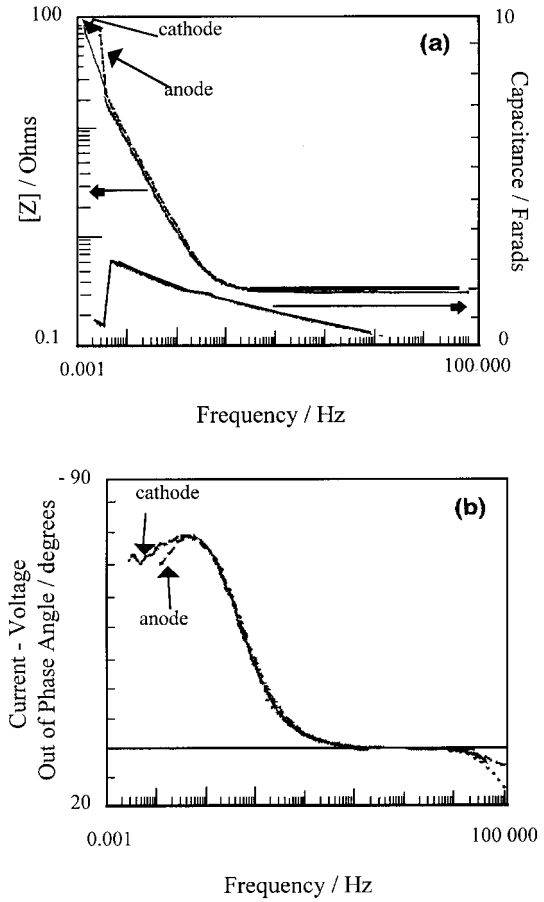

Fig. 5. AC impedance spectroscopy plots of Mo_xN electrodes contaminated with MoO_2 on Ti substrates in 4.4 M H_2SO_4 and biased at +0.69 V of (a) magnitude of the impedance [*Z*] and capacitance and (b) current–voltage phase against frequency.

where the CV plot is not purely rectangular and has increasing current with potential. The a.c. impedance values were obtained by the calculation of the data points which gives a total capacitance that includes portions that are not included in the rectangular CV capacitance calculations. The slope of the impedance line is (−1) for both the anode and cathode which is typical of a porous capacitive electrode. In addition, neither the anode nor the cathode has a slope change at low frequencies which indicates electrochemical stability. In Fig. 4(b) the voltage and current of the two electrode cell approaches −90° out of phase at low frequencies, which is ideal capacitive behaviour. In Fig. 5(a) an electrochemical reaction is indicated by the splitting of the lines between the Mo_xN anode and cathode on Ti substrates biased at +0.69 V. The capacitance of these electrodes appears to be much larger than those represented in Fig. 4(a), but these values are misleading due to the electrochemical reaction. The slopes of the anode and cathode lines in Fig. 5(a) are not (−1), change rapidly at the lowest frequencies and do not have the same values. Further evidence of the electrochemical reaction in these films is indicated by examining the plot of angular dependence against frequency plot in Fig. 5(b). These films do not approach the ideal capacitor value of −90° but show a sudden decrease in angular dependency at low frequencies.

The plot of the real and imaginary impedance as a function of frequency gives useful information regarding the electrode(s) resistance in the electrolyte. The resistance or equivalent series resistance (ESR) is determined by the intersection of the real and imaginary impedance with the *x* or real axis. This is shown in Fig. 6 for an Mo_xN electrode deposited on a nitrided Ti substrate and biased at 0.0 and 0.69 V vs SHE. The intersection with the real axis indicated that the resistance in 4.4 M H_2SO_4 was ~0.04 Ω. The

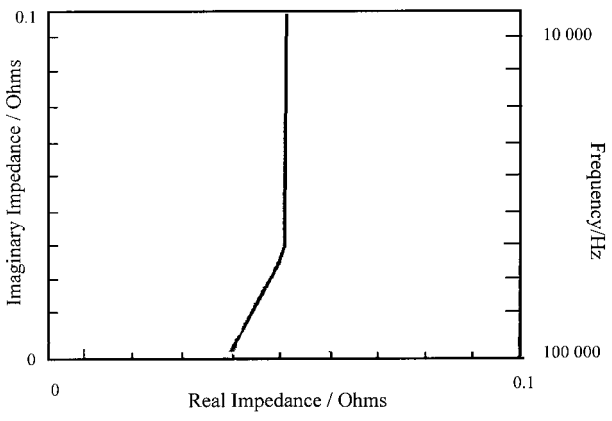

Fig. 6. Real and Imaginary impedance plotted as a function of frequency for Mo_xN films deposited on nitrided Ti substrates and biased at +0.69 and 0 V vs SHE.

slope of the line at high frequencies indicated that the electrodes were porous and the change to a more vertical slope at lower frequencies indicated ideal capacitor resistance behaviour. The values for electrodes biased at 0.0 and 0.69 V overlap. Similar results were also observed for Mo_xN films on bare Ti substrates; however, the ESR for these films were higher, $\sim 0.053\,\Omega$, due to a lower electrical conductivity resulting from MoO_2 contamination in the films.

The bulk effects of electrochemical reactions on the Mo_xN films above their voltage stability limits on a *nitrided* Ti substrate are shown in the XRD patterns in Fig. 7(a) and (b). These patterns indicate the formation of an amorphous product phase. However, there was more amorphous phase (i.e., more electrochemical reaction present) in the positively biased electrode than in the negatively biased electrode. This is indicated by the small peaks present in Fig. 7(a) which correspond to the (200) MoN, (111) γ-Mo_2N, (200) γ-Mo_2N, and (202) MoN, respectively. Although not shown here, there was no discernible difference between the XRD patterns of the reacted Mo_xN films on *nitrided* Ti and Ti substrates.

The results of chemical analyses via SIMS depth profiling of the Mo_xN films on *nitrided* Ti substrates prior to and after exposure to H_2SO_4 at $+0.70$ V are shown in Table 1. There was considerably less nitrogen in the exposed Mo_xN electrodes than in the non-exposed Mo_xN electrodes. There was also much

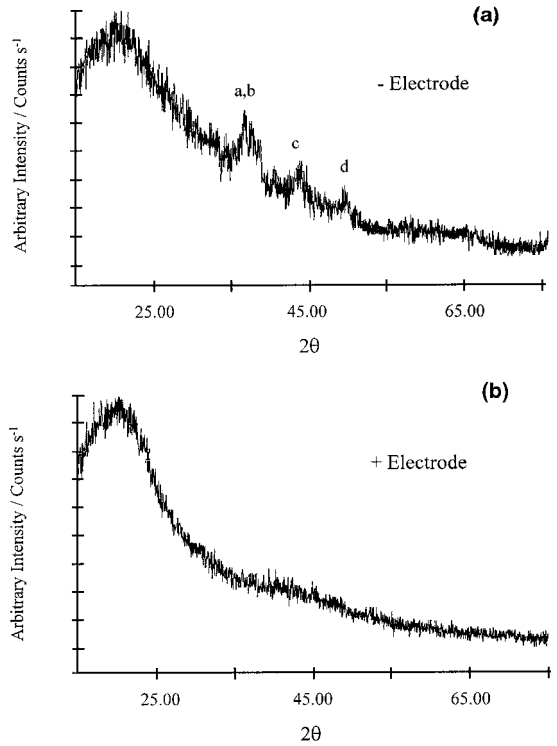

Fig. 7. X-ray diffraction patterns of a (a) negatively biased reacted Mo_xN electrode on a *nitrided* Ti substrate and (b) a positively biased reacted Mo_xN electrode. The peaks in (a) are indexed as follows: (a) (200) MoN, (b) (111) γ-Mo_2N, (c) (200) γ-Mo_2N and (d) (202) MoN.

Table 1. Secondary ion mass spectroscopy data of Mo_xN films on nitrided Ti substrates prior to and after electrochemical reaction during exposure to H_2SO_4 at $+0.70$ V

Elements	*Approximate atomic concentration percentages*		
	Standard	(−) *Electrode*	(+) *Electrode*
Mo	60.02	59.97	59.96
N	39.48	12.00	2.04
O	0.30	26.45	31.97
H	0.10	1.55	2.59
S	0.10	0.03	3.44

less nitrogen present in the electrodes which were positively biased compared to those which were negatively biased. Concentrations of oxygen, hydrogen, and sulfur levels were found in both electrodes, however, they were all higher in the positively biased electrodes. This indicates that nitrogen/oxygen exchange was the principal reaction mechanism in these electrodes. The relatively high concentrations of sulfur, hydrogen, and oxygen and the low concentrations of nitrogen in the positively biased electrodes indicate that Mo_xN is more susceptible to attack by SO_3^- than by H_3O^+. The SIMS data for the Mo_xN films on Ti substrates indicated the same reaction behaviour under positively and negatively bias as the Mo_xN films on the *nitrided* Ti substrates. It should be noted that the concentrations of elements in the nonexposed and exposed electrodes did not vary appreciably as a function of depth and were reproducible; however, all electrodes had slightly greater ($<1\%$) oxygen and hydrogen concentrations on the surface. This is most likely due to the physical adsorption of water and the cleaning of the surface of the films with methanol.

Representative SEM micrographs of a typical Mo_xN film on *nitrided* Ti substrates prior to and after electrochemical exposure between -0.01 and $+0.70$ V are shown in Fig. 8. The large cracks visible on the surface in 8a were observed throughout the volume of the film. These cracks were due to the increase in density of the individual grains during their conversion from MoO_3 to Mo_xN. The microstructure of the positively biased electrode shown in Fig. 8(b) indicates that the cracks around the islands of material became substantially larger as a result of the etching of these areas of higher surface energy. The microstructure of the negatively biased Mo_xN shown in Fig. 8(c) shows that a crack structure similar to that of the unexposed electrode was present after the electrochemical reaction.

Transition metal hydroxides or oxides are usually predicted by Pourbaix diagrams to be the reaction products when their associated metal nitrides are exposed to H_2SO_4. These diagrams for molybdenum indicate that this pure metal is immune to attack or dissolution at negative voltages over the entire pH range [10]. However, at positive voltages, molybdenum dissolves in solvents over the entire pH range, except for the pH range from 5.5 to 7.0 at low volt-

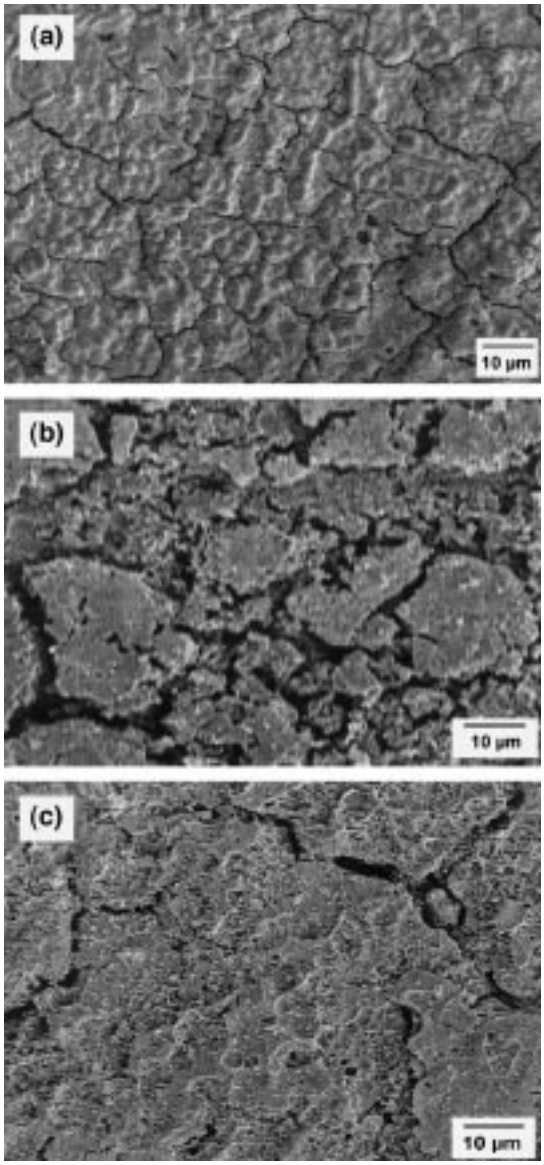

Fig. 8. Scanning electron micrographs of (a) an Mo_xN film prior to reaction, (b) a positively biased electrochemically reacted Mo_xN electrode and (c) a negatively biased electrochemically reacted Mo_xN electrode.

ages where it is passivated to MoO_2. Pourbaix diagrams of molybdenum nitride are not available; however the most likely reaction product of *unbiased* Mo_xN electrodes in H_2SO_4 is either $Mo(OH)_x$ or MoO_x. However, as indicated by Pourbaix diagrams for Mo, $Mo(OH)_x$ is not electrochemically stable at the voltages employed in cyclic voltammetry and a.c. impedance spectroscopy studies used in this research. As shown in Figs 2 and 3, there is a reduction in capacitance between cycles 1 and 50 of electrodes biased at $+0.70$ V. However, after 50 cycles at $+0.69$ V, the electrodes remain capacitive. This indicates that a conductive MoO_x phase is most likely formed on the surface of the electrodes. This explains the decrease in the capacitance between cycles 1 and 50. The negatively biased electrodes have higher levels of nitrogen and some polycrystalline Mo_xN phases present after 50 cycles. This indicates that Mo_xN is less susceptible to H_3O^+ attack when negatively biased than SO_3^- attack when positively biased.

4. Conclusions

The electrochemical voltage stability of Mo_xN ($x = 1$ or 2) electrodes on previously *nitrided* Ti and Ti substrates in a 4.4 M H_2SO_4 electrolyte has been determined to be $+0.70$ V (-0.01 to $+0.69$ V) and $+0.68$ V (-0.01 to $+0.67$ V), respectively. At voltages below $+0.69$, cyclic voltammetry and a.c. impedance spectroscopy showed that Mo_xN electrodes on *nitrided* Ti substrates were capacitive. Above $+0.69$ V an electrochemical reaction of the films was observed. Similar electrochemical behavior was observed in Mo_xN films on Ti substrates; however, these films had less capacitance and a lower voltage stability due to the presence of MoO_2. X-ray diffraction patterns of the reacted films revealed that an amorphous phase had formed. Chemical analysis via SIMS indicated that the amorphous phase of the positively and negatively biased electrodes contained primarily molybdenum and oxygen. Scanning electron micrographs showed that the nonreacted (polycrystalline) and reacted (amorphous) electrodes had similar surface morphologies; however, those of the latter electrodes contained widened cracks.

Acknowledgements

The authors wish to express their appreciation to John Miller and Todd Zeigler of JME, Inc., Shaker Heights, Ohio for the a.c. impedance and cyclic voltammetry data and to Dr A. D. Batchelor, Dr Deiter Griffis and David Ricks at North Carolina State University for SIMS analysis of the films. One of the authors (SLR) acknowledges the continuing support via the US Air Force Palace Knight program.

References

[1] S. L. Roberson, D. Finello and R. F. Davis, *in* 'Electrochemical Synthesis and Modification of Materials', edited by S.G. Corcoran, P.C. Searson, T. P. Moffat, P. C. Andricacos and J. L. Delplancke (Mater. Res. Soc. Symp. Proc., 451, Pittsburgh, PA, 1996), in press.
[2] J. G. Choi, R. L. Curl and L. T. Thompson, *J. Catalysis* **146** (1994) 218.
[3] R. S. Wise and E. J. Markel, *J. Catalysis* **145** (1994) 344.
[4] L. Volpe and M. Boudart, *J Solid State Chem.* **59** (1985) 332.
[5] C. H. Jaggers, J. M. Michaels and A. M. Stacy, *Chem. Mater.* **2** (1990) 150.
[6] V. P. Anitha, S. Major, D. Chandrashekharam and M. Bhatnagar, *Surf. Coat. Technol.* **79** (1996) 50.
[7] P. J. Rudnik, M. E. Graham and W. D. Sproul, *Surf. Coat. Technol.* **49** (1991) 293.
[8] J. G. Choi, D. Choi and L. T. Thompson, *J. Mater. Res.* **7** (1992) 374.
[9] S. L. Roberson, D. Finello and R. F. Davis, *in* 'Nanophase and Nanocomposite Materials II', edited by S. Komarneni, J. C. Parker and H. J. Wollenberger (Mater. Res. Soc. Symp. Proc., 457, Pittsburgh, PA, 1996), in press.
[10] M. Pourbaix, 'Atlas of Electrochemical Equilibria in Aqueous Solutions', (National Association of Corrosion Engineers, Houston, TX, 1974).